EFFECTIVE DETECTION OF SEISMIC EVENTS BY NON-CLASSICAL RECEPTIVE FIELD VISUAL COGNITIVE MODELLING

JING ZHAO[1], HAOJIE LEI[1], YANG LI[1], JINCHANG REN[2]*, GENYUN SUN[3], HUIMINN ZHAO[4], HONGYAN SHEN[1] and DAXING WANG[5]

[1] *School of Earth Science and Engineering, Xi'an Shiyou University, Xi'an 710065, P.R. China. zhaojing@xsyu.edu.cn*
[2] *National Subsea Centre, Robert Gordon University, Aberdeen AB10 7QB, U.K.*
[3] *School of Geosciences, China University of Petroleum (East China), Qingdao 266580, P.R. China.*
[4] *School of Computer Sciences, Guangdong Polytechnic Normal University, Guangzhou 510450, P.R. China.*
[5] *Research Institute of E & D, Changqing Oil-Field Company of CNPC, Xi'an 710018, P.R. China.*

(Received April 9, 2023; accepted July 4, 2023)

ABSTRACT

Zhao, J., Lei, H.J., Li, Y., Ren, J.C:, Sun, G.Y., Zhao, H.M., Shen, H.Y. and Wang, D.X., 2023. Effective detection of seismic events by non-classical receptive field visual cognitive modeling. *Journal of Seismic Exploration*, 32: 385-406.

The detection and up-picking of the seismic events are critical for seismic data analysis and interpretation. Events picking can be used for sequence stratigraphic analysis, reservoir feature extraction, the determining of the subsequent reflection interface, the improving of the SNR and the storage prediction. The research of the events picking is very significant for the seismic exploration. In order to overcome the existing events picking methods have the same sensitivity to noise, we propose a non-classical receptive field visual cognitive method for the events picking up. Vision is an important functional organ for human beings to observe and recognize the world. About 80% of the information obtained by human beings from the outside world comes from the visual system, which fully shows that visual information is huge, and also shows that human beings have a high utilization rate of visual information. How to transfer some typical information processing mechanism and target recognition function of human vision to machine is one of the most important and urgent tasks in the field of computer vision and artificial intelligence. The introduction of computer vision technology into geophysical prospecting is still in its infancy in the field of seismic exploration, our research fill the blank of this field, where the use of visual features to improve the seismic data processing and rapid realization of oil and gas exploration, will become the vane of the future direction of research and development.

As a basic research work in the crossing field, this paper has made a breakthrough in the research methods and ideas, and the research content can be summarized as the following four aspects:

0963-0651/23/$5.00 © 2023 Geophysical Press Ltd.

1. The proposed method implements the function of environmental suppression and spatial enhancement of the bio-visual primary visual cortex, which is applies to the pre-stack seismic data, as pre-stack seismic data contains abundant information such as amplitude and frequency to reflect tiny structures of the formation.
2. The seismic data is preprocessed to obtain the wavelet fusion of the envelope peak instantaneous frequency (EPIF) and the slant stack peak amplitude (SSPA), which can maximum the limit to provide optimal quality data.
3. An adaptive Gabor filter direction selection method is proposed to provide a reliable angle range and improve the recognition rate of filter decomposition. In addition, by adopting an anisotropic environmental suppression method, our method can detect edge variability more accurately than the isotropic method.
4. With the enhanced contour aggregation, cocircular constraint is adopted and combined with the characteristics of low curvature and continuous changing curvature, which is unique to the seismic events, to establish a consistent spatial structure perception model. The events picked by our method is more continuous and accurate than the existing methods, and doesn't require human interaction, which is beneficial for subsequent seismic interpretation and reservoir prediction.

KEY WORDS: non-classical receptive field, events picking, pre-stack seismic data, environmental suppression, spatial enhancement, Gabor filter, cocircular constraint.

INTRODUCTION

The events here are defined as the line of phase peaks or troughs (Lu, 1993). When interpreting seismic records, the event is indicated according to the vibration of similar shapes and the regularity of the occurrence of rules. As the seismic wavelet variation of the events is caused by the seismic wave propagation process, the detection and up-picking of the events are critical for seismic data analysis and interpretation. Firstly, as the basis of seismic interpretation, events picking, or event detection, can be used for sequence stratigraphic analysis, reservoir feature extraction and storage prediction. The events can represent the seismic waves of different types or strata, and the detection results can be used for tomographic construction and data interpretation. These can be used to represent stratigraphical interfaces of different lithologies, i.e., sedimentary interfaces, and isochronous stratigraphical interfaces of different geohistorical periods (Lu, 1993). Secondly, the detection of the seismic events plays an important role in determining the subsequent reflection interface (Zhao, 2005). Most information collected in the seismic exploration can be found in these events, for example, the self-excitation time of the events can reflect the depth information of the interface to a certain extent, and the shape of the events reflects the propagation velocity information of the seismic waves in the medium (Li, 2014). Thirdly, the extracted edges of the events can well improve the signal-to-noise-ratio (SNR) of the seismic profile. Therefore, the originally collected data can better pave the way for seismic exploration interpretation, which is very effective for the consequent oil and gas exploration and stratigraphic research. The research of the events picking is very significant for the seismic exploration.

According to the features used, existing events picking methods can be roughly divided into four categories. The first is based on the instantaneous

characteristics of the seismic records, such as the maximum amplitude method (Wang et al., 2019), and energy ratio method (Shi et al., 2019; St-Onge, 2011). The second category relies on the global features of the seismic records, such as correlation analysis (Spagnolini, 1991), and constraint direct wave method (Huang et al., 2014; Feng et al., 2019), etc. The third is to use artificial intelligence to pick up the events, such as the artificial neural network (McComack, 1993) pattern recognition method (Bondar, 1992; Zhou and Hu, 1991), etc. The fourth is the edge detection method (Li, 2007) based on image processing, which is cutting-edge in seismic exploration (Ning et al., 2007) and becomes increasingly popularly, such as the Sobel operator (Tabatabai et al., 1984), the Canny operator (Canny, 1986) and others. The Canny operator has been widely applied in the scientific community due to its high efficiency and good performance in image edge detection. However, it suffers from a much higher computational cost than that of the derivation-based algorithms, which has constrained its practical applications in real-time seismic data processing (Xiong et al., 2009). The edge detection method actually converts the amplitude value of each sampling point of a 2D seismic signal to different grayscale values, where each seismic channel set is regarded as a grayscale image. In this way, the events in the image can be detected using edge detection method in image processing (Haralick, 1984). Due to the limited spatial resolution and noise, the events information being picked up can be relatively inaccurate. Neural network methods (Glinsky, 1991) use known events as standard samples to train a model whilst minimizing a training error, though sufficient number of samples are often requested, where can be unrealistic especially in selecting the useful samples from the noisy ones. Any newly adopted samples may affect the trained model, where the lengthy iterative process will also cause heavy computational cost. In seismic exploration, due to different locations of the two adjacent receiving points and the fluctuation of the underground interface, the time of the reflection wave caused by the same source reflecting the same underground reflection interface becomes different in the two adjacent traces. The basic principle of the cross-correlation method (Ding et al., 2012) is to extract the events susceptible to noise, based on the waveform similarity of the events between seismic traces. The maximum of the correlation coefficient can be obtained by analyzing one of the wave with the other after a delay of t_0, where the spatial resolution decreases with the increasing time delay. In the chain matching method, each waveform is represented by links of peaks and valleys which have multiple features, where the picking of events is transformed into the problem of optimal matching between chains, i.e. finding the shortest link path. This method is sensitive to the interference of noise, space and frequency, so it is also difficult to solve the complex events processing problem. Tu et al. (1993) proposed an automatic events picking system, which includes three steps, i.e. two-dimensional matched filter, Kalman filter and flexible template. Matched filtering is used to detect targets, Kalman filter eliminates random interference and recovers data from noise.

In short, these existing algorithms have the advantages of fast speed and simple implementation. But these methods are used to events contour

feature extraction under low SNR, often have the same sensitivity to the noise, so as to also detect the outline of the noise when they detect the event edges, lead to low efficiency of the events detection. Vision is an important functional organ for human beings to observe and recognize the world. About 80% of the information obtained by human beings from the outside world comes from the visual system, which fully shows that visual information is huge, and also shows that human beings have a high utilization rate of visual information. Human vision has extraordinary environmental perception and cognitive ability, and it seems to be effortless to identify typical objects in the surrounding environment. The high intelligence and high efficiency of human vision has aroused great interest of neuroscientists. With the deep understanding of human vision system, enhancing the cognitive ability of machine vision through the information processing mechanism of human vision has become one of the hot topics in the field of computer vision (Jin, 2010). Biological visual primary visual cortex (V1) can inhibit environmental information and enhance the cyclic excitation of the target, so that the visual cortex can quickly and efficiently extract the contour or boundary of the object from the complex environment, and provide important feature information for the subsequent visual cognition. Therefore, the construction of computational methods with biological visual cortex functional characteristics is one of the effective methods to achieve target contour extraction under complex conditions, and also one of the key technologies to achieve target recognition. With the development of related disciplines, the research results of the computer vision are shocking (Wang et al., 2018). Grossberg and his colleagues (Grossberg and Mingolla, 1984) have been working on building the model of the function of the visual cortex and structure for the past several decades, and have made many important contributions to the modeling of the visual cortex (Grossberg and Carpenter, 2003). Chang and Chatterjee (1993), Folsom and Pinter (1998), Milanova et al. (2000), etc. verified that Gabor function has the function of simple cells in visual cortex and can better simulate the orientation sensitivity of simple cells. Also, the two-dimensional Gabor function can approximately simulate the characteristics of simple cell receptive fields in the mammalian visual cortex (Petkov and Wieling, 2008). These biological visual cortex functions provide a good inspiration for record edge detection in computer vision (Petkov and Wieling, 2017).

How to transfer some typical information processing mechanism and target recognition function of human vision to machine is one of the most important and urgent tasks in the field of computer vision and artificial intelligence (Petkov, 1995). Visual cognition is utilized for seismic data processing, according to the picking of the events of the seismic reflection profile to explain the influence of the structure, through the picking of the events of the seismic profile to determine the location of the effective oil and gas in stratigraphic, and then realize the seismic data processing and interpretation by the effective stratigraphic position information to improve the efficiency of seismic exploration. For the extraction of the profile features of the seismic events, this paper proposes a new method of implementing a contour and boundary detection model based on the

perception mechanism of the primary visual cortex. The frequency and direction representation of Gabor filters are close to that of the human visual system, and they are often used for texture representation and description. In the field of image processing, Gabor filter is a linear filter used for edge detection (Grigorescu et al., 2002). In this paper, the simple receptive field profile of the mammalian visual cortex is represented by a group of Gabor functions, and the excitation and inhibition mechanism of non-classical receptive field is used to reduce the background noise and highlight the boundary of the region. Finally, the contour is refined by non-maximum suppression and the binarized contour is extracted by hysteresis threshold method. The proposed non-classical receptive field visual cognitive model can perform effective detection of events' edges on the target contour image with huge data and heavy noise. Compared with other traditional methods, the proposed computational model with visual environment inhibition and spatial enhancement can make the seismic events edge detection more advantageous and be more consistent with the biological vision mechanism. The events picked by our method is more continuous and accurate than the existing methods, providing a new research direction for future seismic data interpretation.

Therefore, it is necessary to discuss how to extract the events of interest based on visual features. The introduction of computer vision technology into geophysical prospecting is still in its infancy in the field of seismic exploration, where the use of visual features to improve the seismic data processing and rapid realization of oil and gas exploration, will become the vane of the future direction of research and development.

METHOD

The events are defined as the connection of the phase peak (wave peak or trough), and the events picking is the basis of seismic interpretation, which can be used in the study of sequence stratigraphy, reservoir prediction and storage feature extraction. In this paper, events picking is based on the pre-stack seismic data, which contains more abundant information than post-stack seismic data, not NMO stretching and stacking, non-damaged amplitude and frequency information, which can reflect some subtle stratigraphic features though possibly suffer from a low signal-to-noise ratio (SNR) and more noise.

Therefore, in view of the low SNR of the pre-stack seismic data, this paper proposes a high-precision events picking method. Assuming that the source wavelet can be approximated by the following constant phase wavelet with four parameters:

$$s(0,t) = A'(\frac{\delta^2}{\pi})^{1/4} \exp[i(\sigma t + \phi) - (\delta t)^2 / 2] \quad , \tag{1}$$

where σ is the Modulated angular frequency, δ is the energy attenuation factor, A' and ϕ are the amplitude and the phase, respectively.

By conducting the Fourier transformation on both sides of eq. (1), we

have:

$$S(0,\omega) = A\left(\frac{4\pi}{\delta^2}\right)^{1/4} \exp\left[-\frac{(\omega-\sigma)^2}{2\delta^2} + i\varphi\right] \quad . \tag{2}$$

According to Barnes' definition, the envelope peak instantaneous frequency (EPIF) of the constant-phase wavelet is the average frequency weighted by the wavelet amplitude spectrum to the Fourier frequency, i.e.,

$$f_p(\tau) = \frac{\int_0^\infty fS(\tau, f)df}{\int_0^\infty S(\tau, f)df} \tag{3}$$

The EPIF of the zero-time source wavelet is obtained by substituting the mode of eq. (2) into eq. (3):

$$f_p(0) = \frac{\sigma}{2\pi} + \frac{\dfrac{\delta^2}{2\pi^2}\exp\left[-\dfrac{2\pi^2}{\delta^2}\left(\dfrac{\sigma}{2\pi}\right)^2\right]}{\int_0^\infty \exp\left[-\dfrac{2\pi^2}{\delta^2}\left(f-\dfrac{\sigma}{2\pi}\right)^2\right]\mathrm{d}f} \tag{4}$$

The peak amplitude of the slant stack is calculated based on the instantaneous amplitude as follows:

$$A(t) = \left|s(t) + i\cdot H\left[s(t)\right]\right| \tag{5}$$

where

$$H\left[s(t)\right] = \mathrm{Im}\left[\int_{-\infty}^{\infty} S(b,a)a^{-1}da \Big/ \int_0^\infty \hat{g}_R(\omega)\omega^{-1}d\omega\right]$$

is the analytic part of the signal calculated by wavelet transformation, $A(t)$ is the magnitude of the instantaneous amplitude, s(t) is a trace of seismic data, S(b,a) is wavelet transform of seismic data, $\hat{g}_R(\omega)$is the real part of Fourier transform of the wavelet function g(t), a is the scale factor, b is the shift factor, The wavelet transform of s(t) is defined as:

$$S(b,a) = \frac{1}{a}\int_{-\infty}^{+\infty} s(t)\bar{g}\left(\frac{t-b}{a}\right)dt \tag{6}$$

where, $t,b\in\mathbf{R}$, $a>0$; $g(t)\in L^1(\mathbf{R},dt)\mathrm{I}\ L^2(\mathbf{R},dt)$, $\bar{g}(t)$is the Complex conjugate of $g(t)$.

The Slant stack is the local Radon transform. This paper uses a local linear Radon transformation. The integral path of the linear Radon transform is linear, also known as the $\tau - p$ transform, and its discrete form in the frequency domain is:

$$M(f,p)=\sum_{m=1}^{nx}\hat{A}(f,x_m)e^{j2\pi fpx_m} \tag{7}$$

where $M(f,p)=\int m(\tau,p)e^{-j2\pi f\tau}d\tau$, $\hat{A}(f,x_m)=\int A(t,x_m)e^{-j2\pi ft}dt$ is the Fourier transformation of the instantaneous amplitude $A(t,x_m)$, x_m is the reference trace, $m(\tau,p)$ is the Radon transformation in the time domain.

The calculation process of local linear Radon transform is given in Fig.1. For a selected reference trace on the instantaneous amplitude section, τ_i denotes certain time intercept, where several traces near the reference trace are superimposed along n_p straight lines with different slopes p_j ($j=1,2,\mathrm{L},n_p$) (slope in interval sampling Δp). The sum of the instantaneous amplitude along different directions at the time intercept is recorded in the corresponding position (τ_j,p_j) of the coordinate axis $\tau-p$. When the selected stacking slope is close or equal to the slope of the events, records in the t-x domain becomes the maximum. Putting the average of the maximum stacking values on the corresponding position (τ_i,x_m) in the t-x domain (time-distance domain), a super-gather can be constructed to increase the SNR, which is called the slant stack peak amplitude (SSPA) profile. Also, the slope corresponding to the maximum stack value is placed at the corresponding position in the t-x domain to form a gradient profile. Among many methods for calculating the linear Radon transform, we use the frequency-spatial domain matrix multiplication algorithm (Stankovic et al., 2001) for its high precision. Before performing the Radon transform, the instantaneous amplitude data in the time domain is zeroed out to increase the frequency resolution. In this paper, the zeroed-out length is three times of the data length.

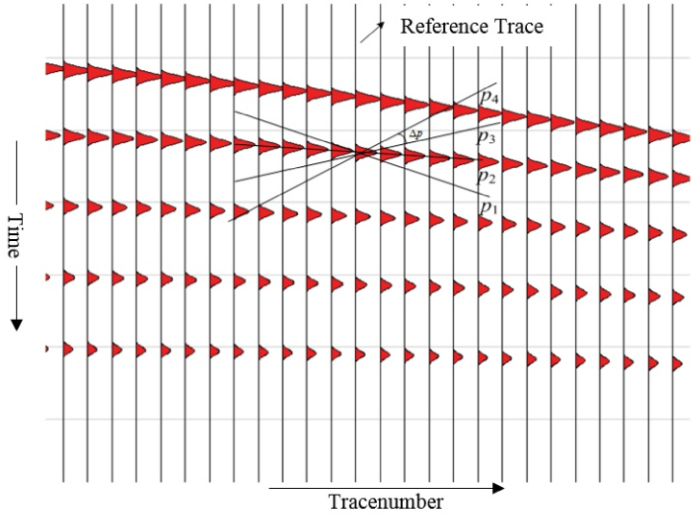

Fig.1. The calculation process of local linear Radon transform.

So far, the envelope of the peak instantaneous frequency and the SSPA have been obtained. Then, the wavelet fusion of the two is achieved as follows. Let $f(t_1,t_2)\in L^2(R^2)$ represent a two-dimensional signal on R^2, where t_1 and t_2 of $f(t_1,t_2)$ denote respectively the coordinate and ordinate. $\psi(t_1,t_2)$ is the 2D mother wavelet. After resolution stretching and displacement, the definition of the two-dimensional continuous mother wavelet is as follows:

$$\psi_{a,\tau_1,\tau_2}(t_1,t_2)=\frac{1}{a}\psi(\frac{t_1-\tau_1}{a},\frac{t_2-\tau_2}{a}) \tag{8}$$

Then, the two-dimensional continuous wavelet transform is given by:

$$WT_f(a;\tau_1,\tau_2)=\left\langle f(t_1,t_2,\psi_{a;\tau_1,\tau_2}(t_1,t_2)\right\rangle =\frac{1}{a}\iint f(t_1,t_2)\psi(\frac{t_1-\tau_1}{a},\frac{t_2-\tau_2}{a})dt_1dt_2 \tag{9}$$

where $1/a$ is the normalization factor, which can ensure the conservation of energy before and after the wavelet stretching. In order to realize the 2D wavelet transform digitally, two-dimensional wavelet discretization (DPWT) is implemented to induce the two-dimensional discrete wavelet transform as follows:

$$DPWT(j,k_1,k_2)=a_0^j\iint f(t_1,t_2)\psi(a_0^jt_1-k_1\tau_{10},a_0^jt_2-k_2\tau_{20})dt_1dt_2 \tag{10}$$

where, in the 2D continuous wavelet, $a=a_0^j$, $\tau_1=a_0^jt_1k_1\tau_{10}$, $\tau_2=a_0^jt_2k_2\tau_{20}$, $j,k_1,k_2\in Z$, a_0, τ_{10}, τ_{20} are all constants. The wavelet transform in two-dimensional discrete space (DSWT) can be obtained after the integral is discretized and then series, as shown in the formula below:

$$DSWT(j,k_1,k_2)=a_0^j\sum_m\sum_n f(m,n)\psi(a_0^jm-k_1\tau_{10},a_0^jn-k_2\tau_{20}) \quad . \tag{11}$$

Finally, the two-dimensional discrete wavelet transform can be obtained after the special case of the two-dimensional discrete space wavelet transform, as shown in the formula below:

$$DWT(j,k_1,k_2)=2^j\sum_m\sum_n f(m,n)\psi(2^jm-k_1,a_0^jn-k_2) \quad , \tag{12}$$

where we set $a_0=2$, $\tau_{10}=\tau_{20}=1$.

Two-dimensional image fusion based on the wavelet transform is mainly divided into three steps:

(1) Each original image to be fused is decomposed by wavelet transform to obtain the decomposition coefficients in different directions;

(2) The coefficients in different directions obtained by decomposition are fused;

Fusion has certain rules: 1. Method with large absolute value of coefficients. The function of the wavelet transform is to discorrelate the signal and concentrate all the information of the signal into a part of wavelet coefficients with large values. These large wavelet coefficients contain much more energy than the small coefficients. Therefore, in the signal reconstruction, the large coefficients are more important than the small coefficients. 2. Method of weighted mean. The weight coefficient is adjustable. The advantage is that it can eliminate part of the noise and loss less source image information, but will cause the image contrast drop. 3. Local variance criterion.

Each decomposition layer of wavelet decomposition is fused separately, and different fusion operators are used to fuse different frequency components of each decomposition layer. Finally, the wavelet pyramid after fusion is obtained. For the low frequency we use the weighted average rule, and for the high frequency we use the large absolute value rule.

(3) The final image can be obtained by inverse wavelet transform of the coefficients obtained from fusion.

The image fusion process based on the two-dimensional wavelet transformation is shown in Fig 2.

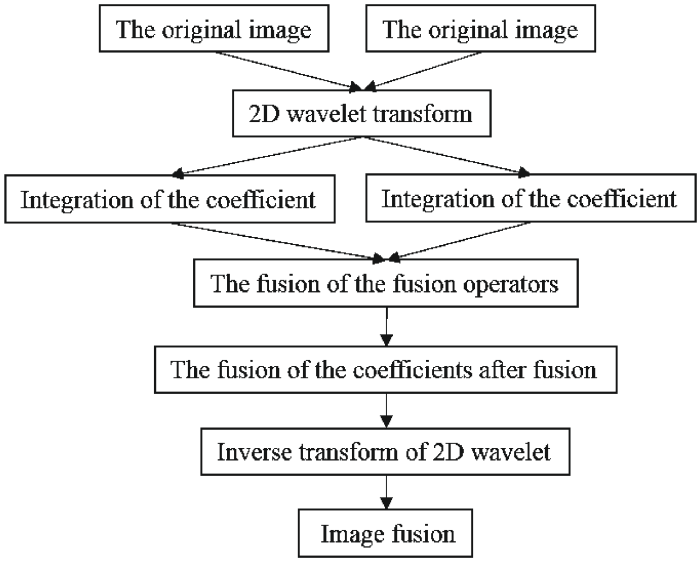

Fig. 2. The image fusion process based on the two-dimensional wavelet transformation.

Gabor function can be expressed as a double function of selective alternation between the feature location of receptive field and its spatial frequency, which can effectively describe the receptive field characteristics of simple cells in the human visual cortex. The two-dimensional Gabor function can approximately simulate the characteristics of simple cell receptive fields in the mammalian visual cortex. It is a Gaussian function modulated by a complex sine function, as given below:

$$g(x,y)=h(x',y')\exp(j2\pi fx') \tag{13}$$

where $\begin{cases} x' = x\cos\theta + y\sin\theta \\ y' = -x\sin\theta + y\cos\theta \end{cases}$, θ is the direction of the filter. Filtering in any direction can be realized through the rotation of the coordinate system, which reflects the selective sensitivity of the cell receptive fields to the particular direction. f represents the center frequency, which determines the effective region of the filter, $h(x,y)$ is the Gaussian function, and its expression is:

$$h(x,y)=\frac{1}{2\pi\sigma_x\sigma_y}\exp\left\{-\frac{1}{2}\left[\left(\frac{x}{\sigma_x}\right)^2+\left(\frac{y}{\sigma_y}\right)^2\right]\right\} \quad , \tag{14}$$

where, σ_x and σ_y are the horizontal and vertical covariance of a Gaussian function respectively.

The traditional Gabor filters adopt fixed directions, such as 0°, 45°, 90°, and 135°, which have a low recognition rate and do not take into account the characteristics of object content and the differences between classes (Zhang et al., 2010). In addition, selecting more fixed directions are not a good solution. Considering the particularity of the events gradient of the seismic data, in this paper, we use the dip profile obtained by the Radon transform to adaptively set the filter direction, which can thus improve the recognition rate and outperform the traditional methods in obtaining the dip profile with the SSPA profile. The dip of the events has continuity, so starting from the first column of the dip angle section can detect the surrounding points around it. By comparing the difference of the amplitude between the surrounding points and the points of the reference trace (for CSP data, this only refers to the right side of the points around for saving the computation), if it is within a given threshold range that is contained in the dip angle of an event, we retain the value of the point; Otherwise, it will be considered as noise and set to zero for removal. The maximum and minimum values will be picked up as the upper and lower limits of the Gabor filter at an interval of 5° after going through all the elements. The reason why the Gabor integral transform is performed at an interval of 5° is to avoid the false directions being generated at a lower angular resolution.

The non-classical receptive field results in the difference of inhibition degree of cell response in different directions and positions of the receptive field. As shown in Fig. 3, the two edges of the triangle in different directions

from the background texture are highlighted, while the edges in the same direction as the background texture are completely suppressed. Therefore, the non-classical receptive field inhibition is the basic feature of biological boundary detection, through which the boundary and isolated contour of the region are largely detected. The seismic events pickup is different from this, as the target to be picked has a consistent or continuous texture, which needs to be highlighted, while the chaotic background noise texture needs to be completely suppressed.

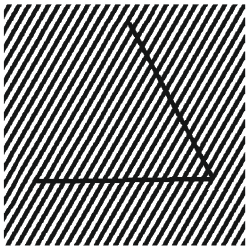

Fig. 3. The principle of the non-classical receptive field inhibition.

Therefore, we refer to anisotropic inhibition characteristics of non-classical receptive field, and the relationship between the inhibition degree and the orientation is expressed by:

$$\Delta\left(x,y,x-x_0,y-y_0\right)=\left|\sin\left(\Theta_\theta\left(x,y\right)-\Theta_\theta\left(x-x_0,y-y_0\right)\right)\right| \tag{15}$$

where, $\Theta_\theta(x,y)$ is the gradient angles of the point (x,y). $\Delta\left(x,y,x-x_0,y-y_0\right)$ is the suppression weights from the point (x,y) to point $\left(x,y,x-x_0,y-y_0\right)$ due to the differences in directions. In addition to direction influence on the degree of inhibition, the distance also affects the degree of inhibition between cells. In this paper, the Gaussian difference function was used to simulate the distance inhibition relationship between cells:

$$w_\sigma\left(x,y\right)=\frac{H\left(DoG_\sigma\left(x,y\right)\right)}{\left\|H\left(DoG_\sigma\right)\right\|} \quad , \tag{16}$$

$$DoG_\sigma\left(x,y\right)=\frac{1}{2\pi\left(4\sigma\right)^2}\exp\left(-\frac{x^2+y^2}{2\left(4\sigma\right)^2}\right)-\frac{1}{2\pi\sigma^2}\exp\left(-\frac{x^2+y^2}{2\sigma^2}\right), H\left(z\right)=\begin{cases}z & z\geq 0\\ 0 & z<0\end{cases},$$

$\|g\|$ is the first order norm of a vector, $w_\sigma(x,y)$ is the distance weighting. The total inhibition of the environment to a given stimulus is:

$$T_o=\sum_i M_i\Delta_{\Theta,\theta}w_\sigma \quad , \tag{17}$$

where i represents the environmental points around the interest points o, and M_i represents the excitatory response of the environmental stimulus points, namely the gray value of pixels or the response value of primary cells.

The Gestalt perception criterion (Yan et al., 2018) tells us that vision can aggregate the local features which has the characteristics of the consistency rule into a whole, enabling objects to highlight from a complex background. The co-occurrence constraint determines a local aggregation function with the greatest likelihood for contour aggregation in natural scenes, which further suggests that the degree to which neurons are enhanced by external environmental stimuli depends on the curvature of the two neuronal preference directions. The seismic events curvature has consistency or continuity, and the smaller the curvature of the cocircular contour is, the stronger the enhancement effect becomes. To reflect the effect of low curvature, the excitation is weighted according to the curvature by the weighted function below:

$$w_c = \exp\left(-\frac{k^2}{\sigma^2}\right) \quad , \tag{18}$$

where,

$$k = \frac{1}{r} = \frac{1}{d}\sin\theta = \begin{cases} \frac{2}{d}\sin\left|\frac{\beta-\alpha}{2}\right|, 0 \le 2\gamma-\alpha < \pi \\ \frac{2}{d}\cos\left|\frac{\beta-\alpha}{2}\right|, 2\gamma-\alpha < 0 \text{或} 2\gamma-\alpha \ge \pi \end{cases}$$ is the curvature,

$d = \sqrt{(x'-x)^2 + (y'-y)^2}$ is the distance between the two neurons,

$\sigma = 0.3$ is the constant, α and β are the preferred orientation of two neurons, γ is the orientation of the connection between two neurons. The exponential function is attenuated, and, therefore, the smaller the curvature is, the greater the weight will be.

Then, the neuron at the center (x', y') of the receptive field, whose gradient direction angle is α, receives enhanced input from the neurons of the external environment as:

$$S(x, y, \alpha) = \sum_{(x', y', \beta)} w_c(x', y', \beta; x, y, \alpha) M(x', y', \beta) \quad , \tag{19}$$

where, $M(x', y', \beta)$ is the response value of the neuron at the point (x', y'), β is the preference orientation angle of the neuron at the point (x', y'), namely, the gradient direction angle of this pixel point.

In order to obtain a clear binarization result, the non-maximum inhibition and the hysteresis thresholding method of the Canny edge detector are adopted. The principle of non-maximum inhibition refinement is: the region around the point (x, y) can be divided into four neighboring regions, with the gradient direction $\Theta_\sigma(x, y)$ of the point (x, y)

corresponding to the specific area, and compare the gradient values of the point (x, y) with the gradient values of the region (x', y') and (x'', y''). If the gradient value of the point (x, y) is the largest, it will be retained; otherwise, the pixel of the point is set to 0 and will be removed.

The principle of the hysteresis threshold, based on two thresholds γ_A and γ_B, where $\gamma_A = \beta \cdot \gamma_B (0 < \beta < 1)$, is to remove noise whilst maintaining the continuity of edges, i.e. edge tracking. First, the edge pixels larger than the threshold γ_B are called quasi-contour point and reserved as image B. The pixels less than γ_A are called non-contour points and should be removed. The pixel values between γ_A and γ_B are the candidate contour points, and the filtered image is A. Contour line tracking is performed from one point in image B, and if there are pixel values in image A contained in this tracking path, the corresponding point in image A is considered as contour line and is reserved. Otherwise, the points outside the tracking line are removed to realize the connection of the edges.

The flowchart of events detection based on the non-classical receptive field inhibition is shown in Fig. 4, which combined the environment suppression and the contour aggregation.

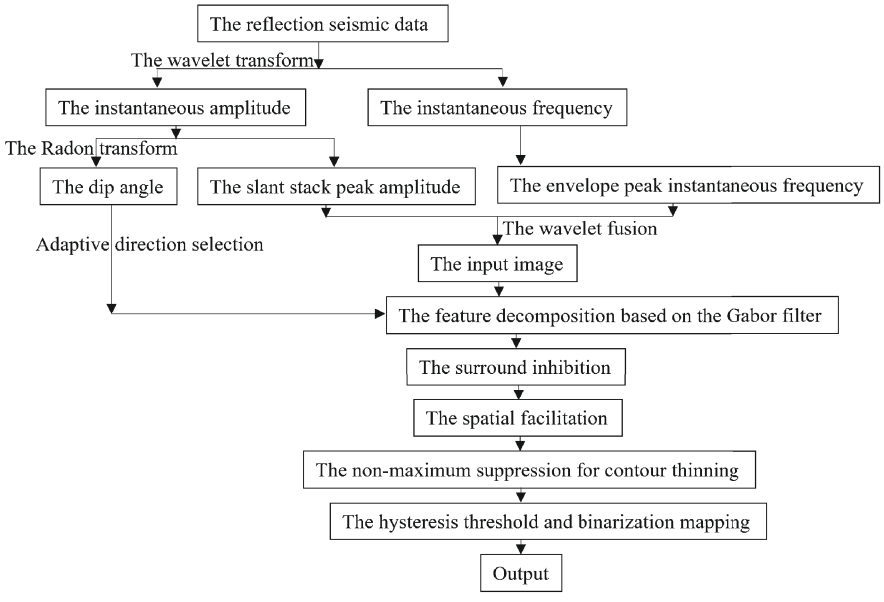

Fig. 4. Flowchart of events detection based on the non-classical receptive field inhibition.

EXAMPLES

Data set 1: synthetic CSP data with Gaussian noise

The proposed method is validated by using a synthetic common shot gather (CSP). The CSP data is synthetized by the finite difference method.

Fig. 5 shows the synthetic data which has the direct wave and the reflection wave. There is a fault on the reflecting interface. We add noise to the data at a SNR of 5. Fig. 6 is the synthetic seismic section with Gaussion white noise. Fig. 7 and Fig. 8 are the instantaneous amplitude (IA) and instantaneous frequency (IF) based on the noised data individually. From Fig. 6 and Fig. 7 we can see that the weak reflection waves are buried in noise. Fig. 9 is the result of the events detection from the visual cognitive method. The direct wave and the reflection wave events are continuous and accurate. The experimental result show that the proposed method has well anti-noise ability.

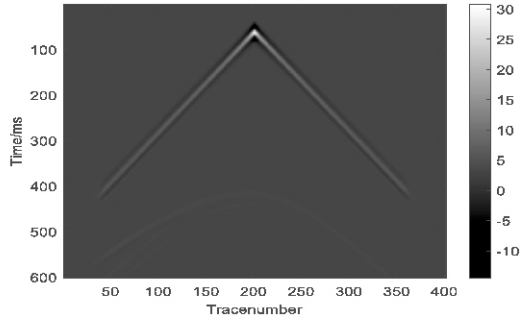

Fig. 5. The synthetic CSP data.

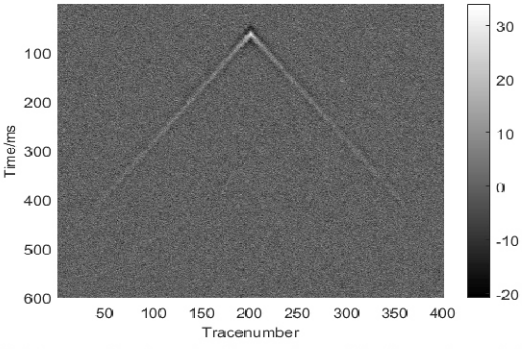

Fig.6. The synthetic seismic section with Gaussian white noise.

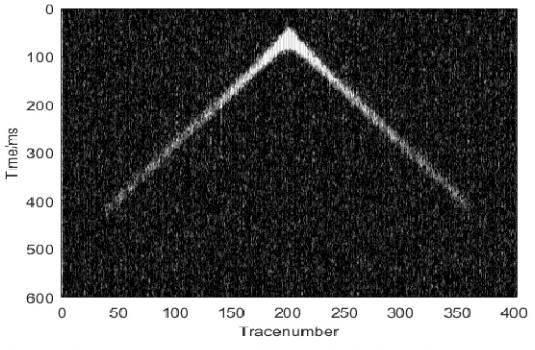

Fig. 7. The instantaneous amplitude (IA) based on the noised data.

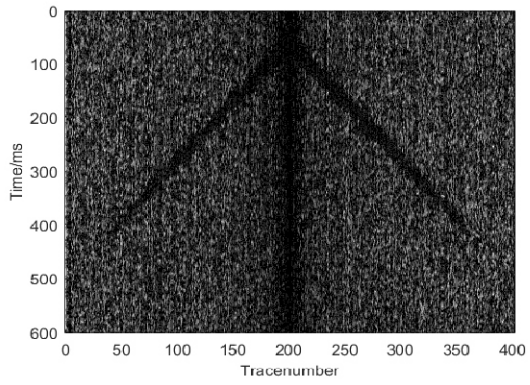

Fig. 8. The instantaneous frequency (IF) based on the noised data.

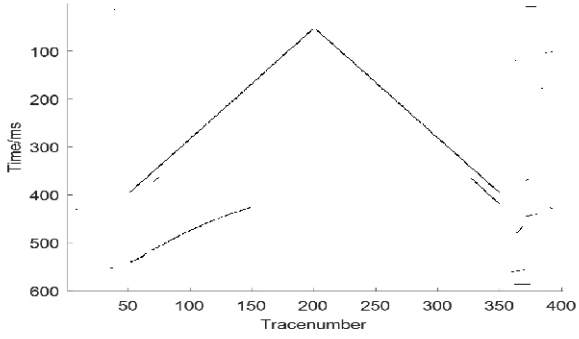

Fig. 9. The result of the events detection from the visual cognitive method.

Data set 2: real field reflection record

To validate the efficacy of the proposed method, we apply it to a real CSP with 595 traces, the minimum offset of 90 m, the distance of 10 m between offsets, 1250 sampling points, and 2 ms sampling. Fig. 10(a) is the original pre-stack seismic data, which contains obvious events, although the background noise is also very large. In particular, the events at the near offset and shallow surface cannot be distinguished, as the peaks and valleys of the events affect each other, which is not conducive to picking up other attribute information such as dip angles. Fig. 10(b) is the instantaneous amplitude (IA) profile. Fig. 11 is the envelope peak instantaneous frequency (EPIF) profile, in which the envelope peak instantaneous frequency reduces the mutual interference between peaks and valleys. Also, the information is further concentrated, but the deep noise is still very large. Fig. 12 shows the wavelet fusion results of EPIF and SSPA profile, where the fused image highlights the events and weakens the impact of noise. Fig. 13 shows the dip angle profile picked up by the Radon transform. Fig. 14 shows the real part of the Gabor filter, which has 8 directions and 5 scales. Fig. 15(a) shows the results of events picking by using the proposed method, in which the

directions are set as 90° - 180° at an interval of 5°. Fig. 15(b) is also the result with different parameters. The directions are set as 0°, 30°, 60°, 90°, 120°, 150°.

The noise (For example, circling by red and green ellipses.) is more than that in Fig. 15(a). The events picking is relatively complete in the shallow layer. However, the events picking is less in the deep layer due to the large noise, and the information is submerged in the noise, but the events picking is completely picked up in the thick layer, indicating the effectiveness of the proposed method in this paper. Fig. 16 shows the result by the automatic events extraction method proposed by Zhao (Zhao et al, 2019). The auto events picking method detects the up and down boundaries of each event, and the final result need human interaction. Fig. 17 shows the non-maximum suppression result by Canny operator. Fig. 18 shows the events detection result by Canny and Sobel operators. We can see that the results have strong noise and disturbance, and the events are not as complete as the visual cognitive method.

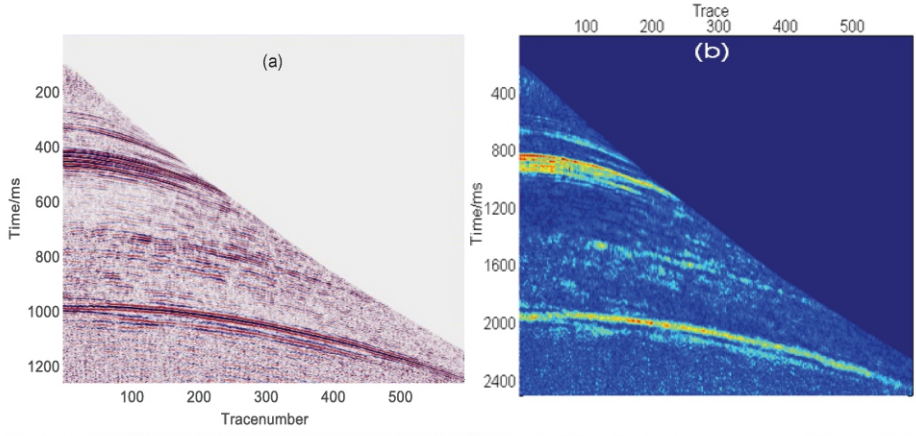

Fig.10. (a) The original pre-stack seismic data. (b) The instantaneous amplitude (IA) data.

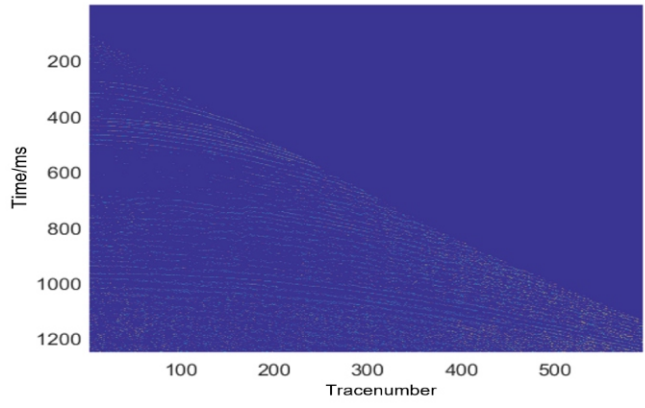

Fig. 11. The envelope peak instantaneous frequency (EPIF) profile.

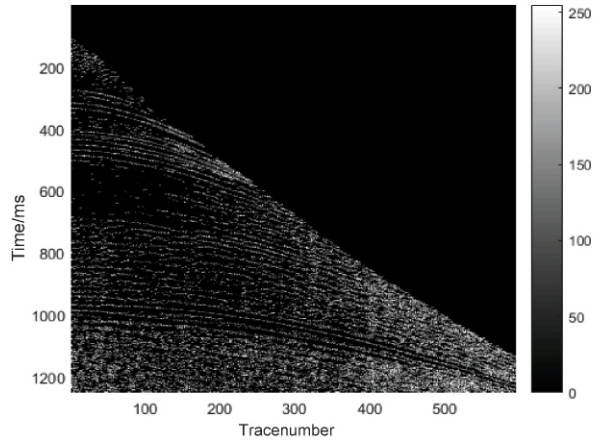

Fig.12. The wavelet fusion results of EPIF and SSPA profile.

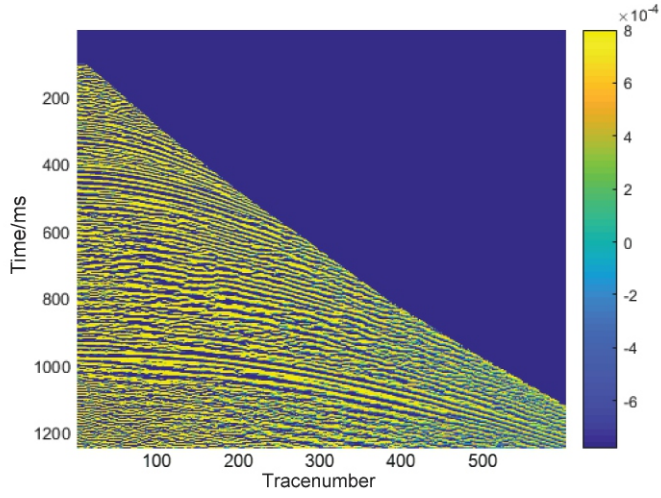

Fig.13. The dip angle profile.

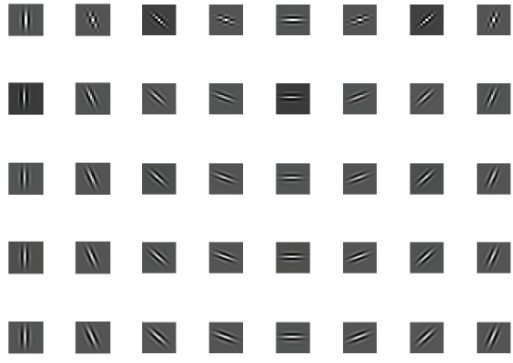

Fig.14. The real part of the Gabor filter.

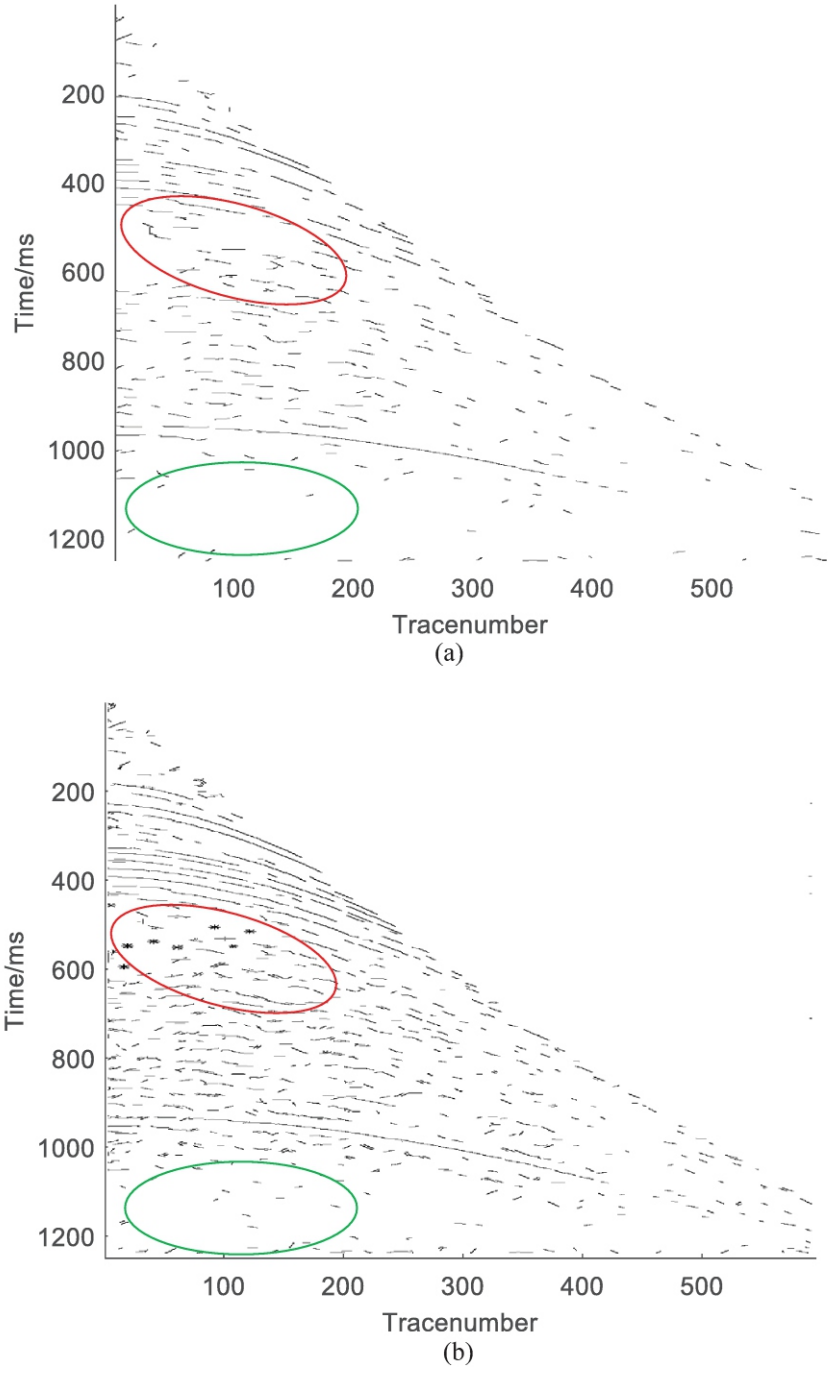

Fig.15. The results of events picking by using the proposed method: (a) The directions are set as 90° - 180° at an interval of 5°. (b) The directions are set as 0°, 30°, 60°, 90°, 120°, 150°.

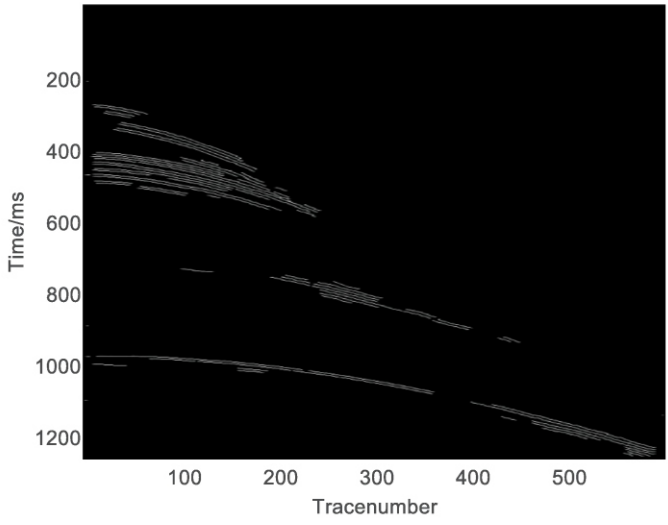

Fig.16. The result by the automatic events extraction method.

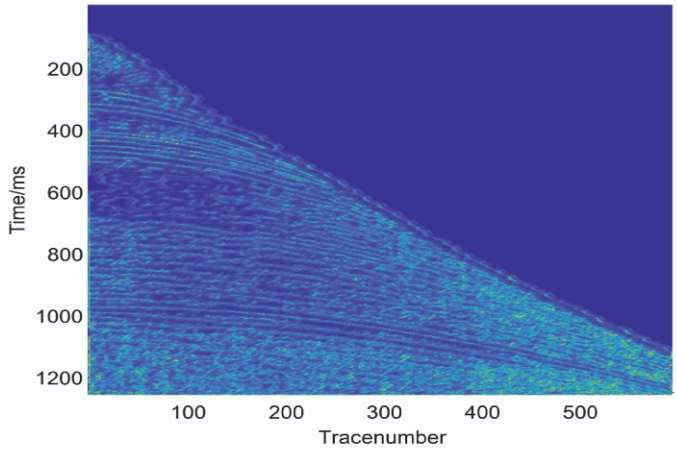

Fig.17. Events detection result by Canny operator.

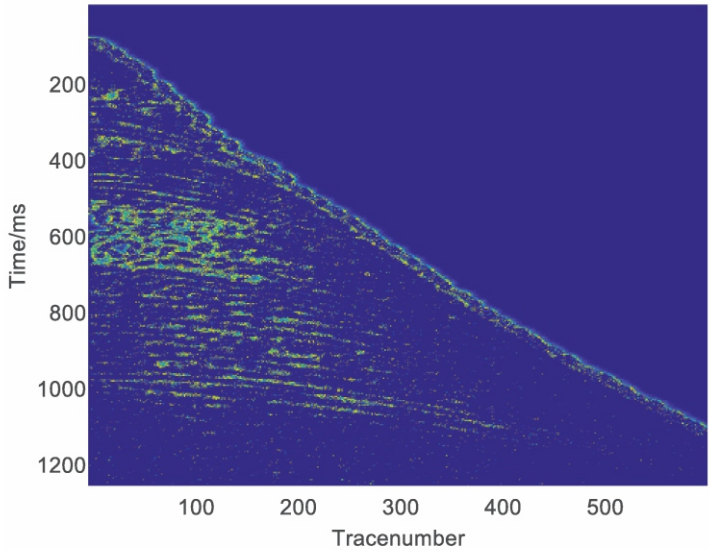

Fig.18. Events detection result by Canny and Sobel operator.

CONCLUSION

In this paper, we propose a method for the events picking up of the seismic data based on environmental suppression and spatial enhancement of the bio-visual primary visual cortex. Our method can enhance the seismic events contour by performing anisotropic suppression of non-related noise, realizing the significant extraction of seismic events contour.

Picking up of the events based on pre-stack seismic data is used, as pre-stack seismic data contains abundant information such as amplitude and frequency to reflect tiny structures of the formation. Firstly, the seismic data is preprocessed to obtain the wavelet fusion of the envelope peak instantaneous frequency and the slant stack peak amplitude, which can maximum the limit to provide optimal quality data. Secondly, an adaptive Gabor filter direction selection method is proposed. Compared with the traditional method, this method can provide a reliable angle range and improve the recognition rate of filter decomposition. In addition, by adopting an anisotropic environmental suppression method, our method can detect edge variability more accurately than the isotropic method. With the enhanced contour aggregation, cocircular constraint is adopted and combined with the characteristics of low curvature and continuous changing curvature, which is unique to the seismic events, to establish a consistent spatial structure perception model. The events picked by the new method is more continuous and accurate than the existing methods, and doesn't require human interaction, which is beneficial for subsequent seismic interpretation and reservoir prediction.

ACKNOWLEDGMENT

This work is partially supported by the Natural Science Foundation of Shaanxi Province, China (2021JQ-587), Innovation and Entrepreneurship Training Program for College Students (S202010705127, X202110705008), Key research and development projects in Shaanxi Province (2022GY-148), National Natural Science Foundation of China (41604113), National Nature Science Foundation Project of International Cooperation (41711530128). We also thank Changqing oilfield for their field data.

REFERENCES

Bondar, A., 1992. Seismic horizon detection using image processing algorithms. Geophys. Process., 40: 785-800.

Canny, J., 1986. A Computational approach to edge detection. IEEE Transact. Pattern Analys. Machine Intellig., PAMI-8(6): 679-698.

Chang, C. and Chatterjee, S., 1993. Ranging through Gabor logonsa consistent, hierarchical approach. IEEE Transact. Neural Netw, 4: 827-843.

Clark, G.A., Glinsky, M.E., Devi, K.R.S., Robinson, J.H. and Ford, G.E., 1996. Automatic event picking in pre-stack migrated gathers using a probabilistic neural network. Geophysics. 66: 1488-1496.

Ding, W.F., Pan, G., Gou, Z.K., Fu, X.M., Zhang, J. and Hu, T., 2012. The research of interactive auto pickup of seismic events based on energy ratio and cross-correlation. Acta Oceanol. Sinica, 34(3): 87-91.

Feng, W.K., Friedt, J.M., Cherniak, G., Hu, Z.P., Sato, M., 2019. Direct path interference suppression for short-range passive bistatic synthetic aperture radar imaging based on atomic norm minimisation and Vandermonde decomposition. IET Radar, Sonar & Navigation, 13(7): 1171-1179.

Folsom, T.C. and Pinter, R.B., 1998. Primitve features by steering, quadrature, and scale. IEEE Transact. Pattern Analys. Machine Intellig., 20: 1161-1173.

Grigorescu, S.E., Petkov, N. and Kruizinga, P., 2002. Comparison of texture features based on Gabor filters, IEEE Transact. Image Process., 11: 1160-1167.

Grossberg, S. and Mingolla, E., 1985. Neural dynamics of perceptual grouping: textures, boundaries and emergent segmentatios. Percept. Psychophys, 38: 141-171.

Grossberg, S. and Carpenter, G.A., 2003. Adaptive Resonance Theory, Handbook of Brain Theory and Neural Networks, 2nd ed. (M.A. Arbib, ed.), Cambridge, MIT Press: 87-90.

Haralick, R.M., 1984. Digital step edges from zero crossing of second directional derivatives. IEEE Transact. Pattern Analys. Machine Intellig., PAMI-6: 58-68.

Huang, C., Zhang, D.L., Sun, D. and Lan, H.L., 2014. Direct path interference suppression based on zero constraint condition with phase correction. J. Harbin Engineer. Univ., 35: 1224-1230.

Jin, L., 2010. Visual cognition based recognition of objects in natural images. Chongqing University, Chongqing.

Li, H.-X., Liu, C. and Tao, C.H., 2007. The study of application of edge measuring technique to the detection of phase axis of the seismic section. Progr. Geophysics, 22: 1607-1610.

Li, X, 2014. Automatic seismic event pickup using edge measuring technique. Ocean University of China, Qingdao.

Lu, J.M., 1993. Principles of Seismic Exploration. China University of Petroleum Press, Qingdao.

McComack, M.D., 1993. First-break refraction event picking and seismic data trace editing using neural network. Geophysics, 58: 67.

Milanova, M.G., Elmaghraby, A.S., Wachowiak, M.P. and Campilho. A., 2000. A computational model of visual cortex receptive fields using spatio-temporal filters. Proc. 2000 IEEE/EMBS Conf. Informat. Technol. Applicat. Biomed.: 129-134.

Ning, J.-S., Wang, H.-H. and Luo, Z.-C., 2005. Downward continuation of gravity signals based on the multiscale edge constraint. Chinese J. Geophys. (In Chinese), 48: 63-68.

Petkov, N., 1995. Biologically motivated computationally intensive approaches to image pattern recognition. Future Generation Comput. Systems, 11: 451-465.

Petkov, N. and Subramanian, E., 2007. Motion detection, noise reduction, texture suppression and contour enhancement by spatiotemporal Gabor filters with surround inhibition. Biological Cybernetics, 97 (5-6): 423-439.

Petkov, N. and Wieling, M.B., 2017. Gabor filtering augmented with surround inhibition for improved contour detection by texture suppression. Perception, 33(supplement):38c.

Shi, W., Lin, C.H., Wang, W.H. and Gao, Y.L., 2019. A first arrival pickup method of micro-seismic event based on statistic energy ratio using varied time window with double constraints. Geophys. Geochem. Explor., 43: 1064-1073.

Spagnolini. U., 1991. Adaptive picking of refracted first arrivals. Geophys. Prosp., 39: 293-312.

Stankovic, S, Djurovic, I. and Pitas, I., 2001. Watermarking in the space/spatial-frequency domain using two-dimensional Radon-Wigner distribution. IEEE Transact. Image Process. IEEE Sign. Process. Soc., 10(4): 650-8.

St-Onge. A., 2011. Akaike information criterion applied to detecting first arrival times on microseismic data. CSPG CSEG CWLS Convention: 1-5.

Tabatabai, A.J. and Mitchell, O.R., 2009. Edge location to subpixel values in digital imagery. IEEE Transact, Pattern Analys. Machine Intellig., *PAMI-6*(2), 188-201.

Tu, P., Mason, **I.** and Zisserman, A., 1993. An automated system for picking seismic events. Expanded Abstr., 63rd Ann. Internat. SEG Mtg., Washington D.C.: 234-237.

Wang, Z., Ren, J., Zhang, D., Sun, M. and Jiang, J., 2018. A deep-learning based feature hybrid framework for spatiotemporal saliency detection inside videos. Neurocomput., 287: 68-83.

Wang, W., Gao, X. and Liu, X.W., 2019. Applicable comparison among several first arrival time automatic pick-up methods in tunnel advance detection by seismic wave. Tunnel Construct., 39: 1239-1246.

Xiong, H.J., Guan, Y.P. and Yu, Y.J., 2009. Extraction of cophasal axes on seismic sections based on the edge detection method. Progr. Geophys. (in Chinese), 24: 2250-2254.

Yan, Y., Ren, J., Sun, G., Zhao, H., Han, J., Li, X., Marshall, S. and Zhan, J., 2018. Unsupervised image saliency detection with Gestalt-laws guided optimization and visual attention based refinement, Pattern Recognit., 79: 65-78.

Zhang, L., Wan, C., Liu, H., 2010. A method of Gabor filter direction selection using for palmprint recognition. J. South-Central University for Nationalities, 29(4): 77-81.

Zhao, H., 2005. The layer tracking of fault's sides based on the artificial neural networks. Chengdu University of Technology, Chengdu.

Zhao, J., Ren, J.C., Gao, J.H., Tschannerl, J., Murray, P. and Wang, D., 2019. Automatic events extraction in pre-stack seismic data based on edge detection in slant-stacked peak amplitude profiles. J. Petrol. Sci. Engineer., 178: 459-466.

Zhou, G.X. and Hu, Z.C., 1991. An AR-method for automatically tracking sync-phase axis of the seismic cross-section graph. Acta Automat. Sinica, 17(3): 4.